1973

Stability of slopes in anisotropic nonhomogeneous soils, 1972, rev. January 1973 (75-8)

W. F. Chen

N. Snitbhan

H. Y. Fang

STABILITY OF SLOPES IN ANISOTROPIC NONHOMOGENEOUS SOILS

by

W. F. Chen

N. Snitbhan

H. Y. Fang

Fritz Engineering Laboratory
Department of Civil Engineering
Lehigh University
Bethlehem, Pennsylvania

January 1973

Fritz Engineering Laboratory Report No. 355.13

Stability of Slopes in Anisotropic, Non-Homogeneous Soils

by

W. F. Chen[1], N. Snitbhan[2], and H. Y. Fang[3]

ABSTRACT

Key Words: energy dissipation; limit design method; upper bound; plasticity; slopes; slope stability; anisotropy; non-homogeneity; stability; soil mechanics.

The upper bound theorem of the generalized theory of perfect plasticity has been found to be very successful in analyzing the stability of cuttings in normally consolidated clays. However, most soils in their natural states exhibit some anisotropy with respect to shear strength, and some non-homogeneity with respect to depth. It is difficult to obtain the solution based on the classical limit equilibrium analysis with the assumed non-circular failure plane with such soil properties included. This paper establishes

[1]Associate Professor of Civil Engineering, Fritz Lab., Lehigh University, Bethlehem, Pennsylvania.

[2]Graduate student, Department of Civil Engineering, Lehigh University, Bethlehem, Pennsylvania.

[3]Associate Professor of Civil Engineering, Director of Geotechnical Division, Fritz Lab., Lehigh University, Bethlehem, Pennsylvania.

an expression for the factor of safety for a C-φ soil, based on the limit analysis of perfect plasticity which yields a close-formed solution for sections in which the following conditions are considered: (a) log-spiral failure-plane, through and below toe; (b) non-homogeneity and anisotropy of soil with respect to cohesion, C (the variation of internal friction angle, φ with respect to direction and depth is not considered); (c) general slope.

TABLE OF CONTENTS

I. INTRODUCTION

The upper bound theorem of limit analysis has been previously applied to obtain the critical height of a homogeneous, isotropic embankment for the Coulomb yield criterion and the associated plastic stress-strain relations. A rotaional failure mechanism (logarithmic spiral) passing through or below the toe was assumed in the analysis (2,3). These upper bound limit analysis results were found to be in good agreement with the results of the friction circle procedure (one of the limit equilibrium methods).

The following work is essentially an extension of references 2 and 3. Herein, the general problem of the stability of a non-homogeneous, anisotropic slope of the type shown in Fig. 1 is considered. This type of slope is frequently found in engineering practice but design data to assess the critical height of such a slope are very scant. This lack of detailed information is largely due to the difficult procedures in analysis encountered when conventional limit equilibrium method is used. However, as in previous works (2,3) on the stability of slopes, the upper bound technique of limit analysis can be used to obtain the solutions in closed form for the critical height of the generalized problem.

In the following work, the material of the slopes is assumed to obey the Coulomb yield condition and the associated stress-strain relations. The Coulomb yield condition is described by two parameters, namely; cohesion stress, C and internal friction angle, φ. It is further assumed that only the cohesion stress, C is nonhomogeneous and anisotropic. A discussion will therefore be given of the types of nonhomogeneity and anisotropy to be used in the calculations. However, the internal friction angle, φ is assumed to be homogeneous and isotropic throughout the calculations, i.e. a constant value for a given type of slope.

The term "non-homogeneous" soil used in this paper refers to only the cohesion stress, C which is assumed to vary linearly with depth (Fig. 1c). The variation of internal friction angle φ with depth is not considered. Figure 2 shows diagramatically some of the simple cuttings in normally consolidated clays with several forms of cohesion stress distributions being considered previously by several investigators (4, 5, 7, 9, 11).

The term anisotropy is used exclusively herein to describe the variation of the cohesion stress, C with direction at a particular point; the directional variation of the internal friction angle φ is not considered. The anisotropy with respect to cohesion stress, C of the soils has been studied by several investigators (1, 6). It is found that the variation of cohesion stress, C with direction approximates to the curve shown in Fig. (1b). The cohesion stress C_i, with its major principal stress inclined at an angle i with the vertical direction is given by

$$C_i = C_h + (C_v - C_h) \cos^2 i \qquad (1)$$

in which C_h and C_v are the cohesion stresses in the horizontal and vertical directions respectively. The cohesion stresses may be termed as "principal cohesion stresses". The vertical cohesion stress, C_v for example, can be obtained by taking vertical soil samples at any site and being tested with the major principal stress applied in the same direction. The ratio of the principal cohesion stress C_h/C_v, denoted by K, is assumed to be the same at all points in the medium. For an isotropic material, $C_i = C_h = C_v$ and K = 1.0. The angle m as

shown in Fig. 1a is the angle between the failure plane and the plane normal to the direction of the major principle cohesion stress which inclines at an angle i with the vertical direction. This angle, according to Lo's tests, is found to be independent of the angle of rotation of the major principal stress.

The design of the general slope with different sections as shown in Fig. 1, is becoming more notable because the minimum volume of excavated clay is always desirable. Some slope sections have already been investigated by Odenstadt (7).

II. LIMIT ANALYSIS SOLUTION

The upper bound theorem of limit analysis states that a cut in clay shown in Fig. 1 will be collapsed under its own weight if, for any assumed failure mechanism, the rate of external work done by the soil weight exceeds the rate of internal energy dissipation. The upper bound values of the critical height can then be obtained by equating the external rate of work to the internal rate of energy dissipation for any such a mechanism.

Referring to Fig. 1, the region AA'CB'BA rotates as a rigid body about the as yet undefined center of rotation 0 with the materials below the logarithmic spiral failure surface AB remaining at rest. Thus, the surface AB is a surface of velocity discontinuity.

The rate of external work done by the region AA'CB'BA can easily be obtained from the algebraic summation of $\dot{w}_1 - \dot{w}_2 - \dot{w}_3 - \dot{w}_4 - \dot{w}_5$. The terms, $\dot{w}_1$, $\dot{w}_2$, $\dot{w}_3$, $\dot{w}_4$, and $\dot{w}_5$ represent the rates of external work done by the soil weights in the regions OABO, OB'BO, OCB'O, OA'CO, and OAA'O respectively. After some simplification, the total rate of external work done by the soil weight is found to be

$$\gamma \, \Omega \, r_o^3 \, g(\theta_o, \theta_h, D/r_o) \qquad (2)$$

in which γ is the unit weight of the soil and Ω is the angular velocity of the region AA'CB'BA, and the function $g(\theta_o, \theta_h, D/r_o)$ is defined as

$$g(\theta_o, \theta_h, D/r_o) = g_1 - g_2 - g_3 - g_4 - g_5 \qquad (3)$$

in which

$$g_1 = \frac{1}{3(1 + 9\tan^2\phi)} \left\{(3\tan\phi \cos\theta_h + \sin\theta_h) \exp\left[3(\theta_h - \theta_o)\tan\phi\right] - (3\tan\phi \cos\theta_o + \sin\theta_o)\right\}$$

$$g_2 = \frac{1}{6}\frac{L}{r_o}\sin\theta_o\left[2\cos\theta_o - \frac{L}{r_o}\right]$$

$$g_3 = \frac{\alpha_1}{3}\frac{H}{r_o}\left[\cos^2\theta_o + \frac{L}{r_o}\left(\frac{L}{r_o} - 2\cos\theta_o\right) + \sin\theta_o\cot\beta_1\right.$$

$$\left(\cos\theta_o - \frac{L}{r_o}\right) - \frac{\alpha_1}{2}\frac{H}{r_o}\cot\beta_1\left(\cos\theta_o + \frac{L}{r_o}\right.$$

$$\left.\left. - \sin\theta_o\cot\beta_1\right)\right]$$

$$g_4 = \frac{\alpha_2}{3}\frac{H}{r_o}\left\{\left(\cos^2\theta_h + \sin\theta_h\cos\theta_h\cot\beta_2\right)\exp\left[2(\theta_h - \theta_o)\tan\phi\right]\right.$$

$$+ \left(2\frac{D}{r_o}\cos\theta_h + \frac{D}{r_o}\sin\theta_h\cot\beta_2 + \frac{\alpha_2}{2}\frac{H}{r_o}\cos\theta_h\cot\beta_2\right.$$

$$\left.\left. + \frac{\alpha_2}{2}\frac{H}{r_o}\sin\theta_h\cot^2\beta_2\right)\exp\left[(\theta_h - \theta_o)\tan\phi\right] + \left(\frac{D}{r_o}\right)^2\right\}$$

$$g_5 = \frac{1}{6}\frac{D}{r_o}\sin\theta_h\left\{2\cos\theta_h\exp\left[(\theta_h - \theta_o)\tan\phi\right] + \frac{D}{r_o}\right\}\exp$$

$$\left[(\theta_h - \theta_o)\tan\phi\right]$$

From the geometrical relations, the ratios $\frac{H}{r_o}$, $\frac{L}{r_o}$, and $\frac{N}{r_o}$ can be expressed as

$$\frac{H}{r_o} = \sin\theta_h\exp\left[(\theta_h - \theta_o)\tan\phi\right] - \sin\theta_o$$

$$\frac{L}{r_o} = \cos\theta_o - \cos\theta_h\exp\left[(\theta_h - \theta_o)\tan\phi\right] - \frac{D}{r_o} - \frac{H}{r_o}\left(\alpha_1\cot\beta_1\right.$$

$$+ \alpha_2 \cot\beta_2)$$

$$\frac{N}{r_o} = \cos\phi \exp\left[\left(\frac{\pi}{2} + \phi - \theta_o\right)\tan\phi\right] - \sin\theta_o - \frac{H}{r_o}$$

The total rates of internal energy dissipation along the discontinuity log-spiral failure surface AB is found by multiplying the differential area $rd\theta/\cos\phi$ by C_i times the discontinuity in velocity, $V\cos\phi$, across the surface and integrating over the whole surface AB. Since the layered clays possess different values of C_i, the integration is thus divided into two parts as follows:

$$\int_{\theta_o}^{\theta_h} C_i\ (V\cos\phi)\ \frac{rd\theta}{\cos\phi} = \int_{\theta_o}^{\theta_m} (C_i)_1\ (V\cos\phi)\ \frac{rd\theta}{\cos\phi} + \int_{\theta_m}^{\theta_h} (C_i)_2\ (V\cos\phi)\ \frac{rd\theta}{\cos\phi} \qquad (4)$$

The log-spiral angle, θ_m and the anistropic angle, i, are obtained directly from the geometric configuration shown in Fig. 1 and may be written as

$$\sin\theta_m \exp\ (\theta_m \tan\phi) = \sin\theta_h \exp\ (\theta_h \tan\phi)$$

and

$$i = \theta - \frac{\pi}{2} - \phi + m = \theta + \Phi$$

in which

$$\Phi = -\left(\frac{\pi}{2} + \phi - m\right)$$

Referring to equation (1) and geometry of Fig. 1, $(C_i)_1$, and $(C_i)_2$ can be expressed as

$$(C_i)_1 = C\left\{n_o + \frac{(1 - n_o)}{(H/r_o)}\left[\sin\theta \exp\left[(\theta - \theta_o)\tan\phi\right] - \sin\theta_o\right]\right\}$$

$$\left\{1 + \frac{(1 - k)}{k}\cos^2 i\right\}$$

$$(C_i)_2 = C\left\{n_1 + \frac{(n_2 - n_1)}{(N/r_o)}\left[\sin\theta \exp\left[(\theta - \theta_o)\tan\phi\right]\right.\right.$$

$$\left.\left. - \sin\theta_m \exp\left[(\theta_m - \theta_o)\tan\phi\right]\right]\right\}\left\{1 + \frac{(1-k)}{k}\cos^2 i\right\}$$

After integration and simplification, Eq. 4 reduces to

$$\int_{\theta_o}^{\theta_h} C_i\ (V\cos\phi)\ \frac{r d\theta}{\cos\phi} = C\ r_o^2\ \Omega\ q \qquad (5)$$

in which

$$q = q_1 + q_2 + q_3$$

The functions q_1, q_2, and q_3 are defined as

$$q_1 = \left\{\frac{n_o}{\exp(2\theta_o\tan\phi)}\left[\Psi + \frac{(1-k)}{k}\lambda\right]\right\}_{\theta_o}^{\theta_m} + \left\{\frac{n_1}{\exp(2\theta_o\tan\phi)}\left[\Psi + \frac{(1-k)}{k}\lambda\right]\right\}_{\theta_m}^{\theta_h}$$

$$q_2 = \frac{(1-n_o)}{(H/r_o)\exp(3\theta_o\tan\phi)}\left\{\xi - \Psi\sin\theta_o\exp(\theta_o\tan\phi) + \frac{(1-k)}{k}\left[\rho - \lambda\sin\theta_o\exp(\theta_o\tan\phi)\right]\right\}_{\theta_o}^{\theta_m}$$

$$q_3 = \frac{(n_2-n_1)}{(N/r_o)\exp(3\theta_o\tan\phi)}\left\{\xi - \Psi\sin\theta_m\exp(\theta_m\tan\phi) + \frac{(1-k)}{k}\left[\rho - \lambda\sin\theta_m\exp(\theta_m\tan\phi)\right]\right\}_{\theta_m}^{\theta_h}$$

in which

$$\xi = \frac{(3\tan\phi\sin\theta - \cos\theta)}{9\tan^2\phi + 1}\exp(3\theta\tan\phi)$$

$$\Psi = \frac{\exp(2\theta\tan\phi)}{2\tan\phi}$$

$$\rho = \frac{\exp(3\theta\tan\phi)}{2}\left\{\cos 2\Phi\left[\frac{(\cos\theta - 3\tan\phi\sin\theta)}{2(9\tan^2\phi + 1)} + \frac{(\tan\phi\sin 3\theta - \cos 3\theta)}{6(\tan^2\phi + 1)}\right]\right.$$

$$\left. - \sin 2\Phi\left[\frac{(\sin\theta + 3\tan\phi\cos\theta)}{2(9\tan^2\phi + 1)} - \frac{(\sin 3\theta + \tan\phi\cos 3\theta)}{6(\tan^2\phi + 1)}\right]\right.$$

$$+\left[\frac{(3\tan\phi\sin\theta - \cos\theta)}{9\tan^2\phi + 1}\right]\Bigg\}$$

$$\lambda = \frac{\exp(2\theta\tan\phi)}{2}\cdot\Bigg\{\cos 2\Phi\left[\frac{\tan\phi\cos 2\theta + \sin 2\theta}{2(\tan^2\phi + 1)}\right] - \sin 2\Phi$$

$$\left[\frac{\tan\phi\sin 2\theta - \cos 2\theta}{2(\tan^2\phi + 1)}\right]\Bigg\} + \frac{\exp(2\theta\tan\phi)}{4\tan\phi}$$

Equating the total rates of external work, Eq. 2, to the total rates of internal energy dissipation, Eq. 5, one obtains

$$H = \frac{C}{\gamma} f(\theta_o, \theta_h, \frac{D}{r_o}) \tag{6}$$

where $f(\theta_o, \theta_h, \frac{D}{r_o})$ is defined as

$$f(\theta_o, \theta_h, \frac{D}{r_o}) = \frac{H}{r_o}\frac{q(\theta_o, \theta_h, D/r_o)}{g(\theta_o, \theta_h, D/r_o)} \tag{7}$$

The function $f(\theta_o, \theta_h, D/r_o)$ has a minimum and, thus, indicates a least upper bound when θ_o, θ_h, and D/r_o satisfy the conditions

$$\frac{\partial f}{\partial \theta_o} = 0;\ \frac{\partial f}{\partial \theta_h} = 0:\ \frac{\partial f}{\partial D/r_o} = 0$$

Denoting the stability number of the slopes by a dimensionless number N_s, then

$$N_s = \text{Min } f(\theta_o, \theta_h, \frac{D}{r_o})$$

and the critical height becomes

$$H_c \leq \frac{C}{\gamma} N_s \qquad (8)$$

III. NUMERICAL RESULTS

The complete numerical results of the stability number are obtained by the CDC 6400 digital computer. The optimization technique reported in Ref. 8 which is essentially the method of steepest descent is used to minimize the function of Eq. 7 without calculating the derivatives. The method of steepest descent is described in all standard texts on mathematical optimization (see for example Ketter and Prawel, Ref. 10). The results are then compared in Tables 1, 2, and 3 with the existing limit equilibrium solutions.

For the cases of isotropic and homogeneous slopes, the stability numbers are found to be identical to those previously reported in Refs. 2 and 3. The comparison between the limit equilibrium solutions (Ref. 11) and the present analysis is shown in Table 1 for different values of inclined slope angle β and friction angle φ.

Table 2 shows a comparison of stability numbers obtained from the limit equilibrium and limit analysis for anisotropic but homogeneous slopes. The only existing solutions available for comparison were given by Lo for the case $\varphi = 0$ (6). Herein, as in Ref. 6, the value of m is taken to be 55^o and the value of friction angle, φ is

put equal to zero so that the log-spiral failure surface becomes circular. Both results are in good agreement.

For the case of anisotropic and non-homogeneous slopes with the cohesion stress C increasing linearly with depth (Fig. 2b) and internal friction angle, φ is a constant, a slight modification of Eq. 8 is required. Since the term $C_v/\gamma z$ is constant for normally consolidated clays, the factor of safety is, therefore, independent of the height of the slopes. The expression for the stability numbers now becomes

$$N_s = \text{Min } f'(\theta_o, \theta_n, D/r_o) \tag{9}$$

from which

$$f'(\theta_o, \theta_h, D/r_o) = \frac{H}{r_o}\frac{g'}{g}$$

The function g is identical to that of Eq. 3 while the function g' is defined as

$$g' = \frac{1}{(\frac{H}{r_o})\exp(3\theta_o \tan\varphi)} \left\{\xi - \Psi \sin\theta_o \exp(\theta_o \tan\varphi) + \frac{(1-k)}{k}\right.$$

$$\left.\left[p - \lambda \sin\theta_o \exp(\theta_o \tan\varphi)\right]\right\}_{\theta_o}^{\theta_h}$$

The stability factor N_s as defined in Eq. 9, can now be compared in Table 3 with those obtained previously by Lo (6) using the limit equilibrium method for the case $\varphi = 0$. Good agreement is again observed.

Equations 8 and 9 are now used to generate the stability numbers for the values of friction angle φ ranging from 0 to 40 degrees. The stability numbers are given in Tables 4 and 5 for various degrees

of anisotropy with two types of cohesion stress, C distributions: a) constant C_v, and b) C_v increasing linearly with depth. The angle between the failure and major principal planes, denoted by m in Fig. 1a is taken to be $\pi/4 + \varphi/2$.

IV. CONCLUSION

Slope stability solutions based on the upper bound theorem of limit analysis are presented in terms of stability number for anisotropic, non-homogeneous clay slopes. The formulation of the problem is rather simple and the numerical results for the special cases agree well with the existing limit equilibrium solutions. It can be concluded that the upper bound technique of limit analysis provides a convenient and effective method of analysis for stability of slopes. The solutions obtained will be useful in the design of such general slopes. Design charts or tables can be prepared covering a range of soil properties using the existing computer programs.

V. ACKNOWLEDGMENTS

The research reported herein was supported by the National Science Foundation under Grant GK-14274 to Lehigh University. Nimitchai Snitbhan received financial support from the Government of Thailand during his graduate study at Lehigh.

APPENDIX I - REFERENCES

1. Cassagrande, A. and Carillo, N.
   SHEAR FAILURE OF ANISOTROPIC SOILS, Journal of the Boston Society of Civil Engineers, Contributions to Soil Mechanics, 1941-1953, 1954.

2. Chen, W. F., Giger, M. W., and Fang, H. Y.
   ON THE LIMIT ANALYSIS OF STABILITY OF SLOPES, Soils and Foundations, The Japanese Society of Soil Mechanics and Foundations Engineering, Vol. IX, pp. 23-32.

3. Chen, W. F. and Giger, M. W.
   LIMIT ANALYSIS OF STABILITY OF EMBANKMENTS, Journal of the Soil Mechanics and Foundations Division, ASCE, Vol. 97, No. SM1, January 1971, pp. 19-26.

4. Gibson, R. E. and Morgenstern, N.
   A NOTE ON THE STABILITY OF CUTTINGS IN NORMALLY CONSOLIDATED CLAYS, Geotechnique, Vol. 12, No. 3, 1962, pp. 212-216.

5. Hunter, J. H. and Schuster, R. L.
   STABILITY OF SIMPLE CUTTINGS IN NORMALLY CONSOLIDATED CLAYS, Geotechnique, Vol. 18, No. 3, 1968, pp. 372-378.

6. Lo, K. Y.
   STABILITY OF SLOPES IN ANISOTROPIC SOILS, Journal of the Soil Mechanics and Foundations Division, ASCE, Vol. 91, No. SM4, July 1965, pp. 85-106.

7. Odenstad, S.
   CORRESPONDENCE, Geotechnique, Vol. 13, No. 2, 1963, pp. 166-170.

8. Powell, M. J. D.
   AN EFFICIENT METHOD FOR FINDING THE MINIMUM OF A FUNCTION OF SEVERAL VARIABLES WITHOUT CALCULATING DERIVATIVES, Computer Journal, Vol. 7, 1964, pp. 155-164.

9. Reddy, A. S. and Srinivasan, R. J.
   BEARING CAPACITY OF FOOTINGS ON LAYERED CLAYS, Journal of Soil Mechanics and Foundations Division, ASCE, Vol. 93, No. SM2, March 1967, pp. 83-99.

10. Ketter, R. L. and Prawel, P.
    MODERN METHODS OF ENGINEERING COMPUTATIONS, McGraw-Hill, Inc. 1969.

11. Taylor, D. W.
    FUNDAMENTALS OF SOIL MECHANICS, John Wiley and Sons, New York, 1948.

APPENDIX II - NOTATION

C_i = cohesion stress when the major principal stress at failure is inclined at angle i to the vertical (Fig. 1b)

$(C_i)_1, (C_i)_2$ = cohesion stresses at the depths from zero to H and greater than H respectively (Fig. 1)

C_h, C_v = principal cohesion stresses in the horizontal and vertical directions respectively (Fig. 1)

H = vertical height of an embankment

H_c = critical height of an embankment

N = vertical height of the log-spiral failure surface below toe

L = length B'B in Fig. 1

D = length AA' in Fig. 1

i = angle of rotation of major principal stress from vertical, measured clockwise

m = angle between failure plane and the plane normal to the direction of the major principle stress which inclines at angle i with the vertical direction (Fig. 1)

β_1, β_2 = angular parameters of an embankment

α_1, α_2 = depth factor of the slope

θ_o, θ_h = angular variables of a log spiral curve

θ_m = angle of a log spiral curve, see Fig. 1

φ = friction angle of soil

$r_o, r_h, r(\theta)$ = length variables of a log spiral curve

Ω = angular velocity

$V(\theta)$ = discontinuous velocity across the failure plane

N_s = stability factor

γ = unit weight of soil

K = degree of anisotropy = C_h/C_v

z = ordinate measured from top of slope

C = horizontal cohesion stress at the level of the toe (Fig. 1)

n_o, n_1, n_2 = ratio of cohesion stresses at various depth, as shown in Fig. 1

TABLE 1

Comparison of Stability Number, $N_s = \frac{\gamma}{C_v} H_c$ by Methods of Limit Equilibrium and Limit Analysis for an Isotropic and Homogeneous Soil (φ = constant)

FRICTION ANGLE ϕ IN DEGREES	SLOPE ANGLE β IN DEGREES							
	90		70		50		30	
	Limit Equilibrium	Limit Analysis	Limit Equilibrium	Limit Analysis	Limit Equilibrium	Limit Analysis	Limit Equilibrium	Limit Analysis
	ϕ Circle[a]	Log-Spiral	ϕ Circle[a]	Log-Spiral	ϕ Circle[a]	Log-Spiral	ϕ Circle[a]	Log-Spiral
0	3.83	3.82	4.80	4.80	5.52	5.52	5.53	5.53
5	4.19	4.19	5.47	5.47	6.92	6.92	9.13	9.13
20	5.50	5.50	8.30	8.30	13.63	13.63	--	--
30	6.69	6.69	11.48	11.48	24.41	25.41	--	--
40	8.29	8.29	17.15	17.15	71.49	71.50	--	--

[a]Taylor, D. W., Fundamentals of Soil Mechanics, Reference 11

TABLE 2

Comparison of Stability Number, $N_s = \frac{\gamma}{C_v} H_c$ for an Anisotropic but Homogeneous Soil ($\omega = 0$)

Slope Angle (Degree) β	Anisotropy Factor K	Curved Failure Surface	
		Limit Equilibrium	Limit Analysis
		φ Circle*	Log-Spiral
90	1.0	3.83	3.83
	0.9	--	3.81
	0.8	--	3.79
	0.7	--	3.78
	0.6	--	3.76
	0.5	--	3.74
70	1.0	4.79	4.79
	0.9	4.72	4.72
	0.8	4.65	4.65
	0.7	4.58	4.58
	0.6	4.49	4.49
	0.5	4.41	4.41
50	1.0	5.68	5.68
	0.9	5.54	5.54
	0.8	5.35	5.38
	0.7	5.19	5.23
	0.6	5.09	5.09
	0.5	4.85	4.95
30	1.0	--	7.45
	0.9	--	7.20
	0.8	--	6.95
	0.7	--	6.70
	0.6	--	6.45
	0.5	--	6.19

*Lo (6)

TABLE 3

Comparison of Stability Number, $N_s = \frac{\gamma}{C_v} z$ for an Anisotropic and Nonhomogeneous Soil with the Cohesion Stress, C Increasing Linearly with Depth ($\varphi = 0$)

Slope Angle (Degree) β	Anisotropy Factor K	Curved Failure Surface	
		Limit Equilibrium	Limit Analysis
		ϕ Circle*	Log-Spiral
90	1.0	2.00	2.00
	0.9	2.00	2.00
	0.8	2.00	2.00
	0.7	2.00	2.00
	0.6	2.00	2.00
	0.5	2.00	2.00
70	1.0	2.77	2.77
	0.9	2.73	2.73
	0.8	2.69	2.69
	0.7	2.65	2.65
	0.6	2.61	2.61
	0.5	2.50	2.52
50	1.0	3.78	3.78
	0.9	3.66	3.66
	0.8	3.56	3.56
	0.7	3.45	3.45
	0.6	3.31	3.31
	0.5	3.17	3.20
30	1.0	5.50	5.50
	0.9	--	5.22
	0.8	5.00	5.00
	0.7	--	4.69
	0.6	--	4.41
	0.5	4.18	4.16

*Lo (6)

TABLE 4

Stability Number $N_s = H_c \left(\frac{\gamma}{C_v}\right)$ by Limit Analysis for an Anisotropic but Homogeneous Soils

(φ = constant)

Slope Angle (Degree) β	Aniso-tropy Factor K	Stability Number N_s				
		Friction Angle (Degree) ϕ=0 (m=45°)	Friction Angle (Degree) ϕ=10 (m=50°)	Friction Angle (Degree) ϕ=20 (m=55°)	Friction Angle (Degree) ϕ=30 (m=60°)	Friction Angle (Degree) ϕ=40 (m=65°)
90	1.0	3.83	4.58	5.50	6.78	8.52
	0.9	3.82	4.57	5.49	6.75	8.49
	0.8	3.81	4.56	5.48	6.73	8.46
	0.7	3.79	4.54	5.47	6.70	8.42
	0.6	3.78	4.53	5.45	6.67	8.39
	0.5	3.76	4.51	5.44	6.65	8.39
70	1.0	4.79	6.24	8.29	11.48	17.22
	0.9	4.72	6.20	8.24	11.42	17.13
	0.8	4.65	6.15	8.18	11.35	17.04
	0.7	4.58	6.09	8.12	11.28	16.94
	0.6	4.49	6.03	8.06	11.21	16.85
	0.5	4.41	5.97	7.99	11.14	16.75
50	1.0	5.68	8.51	13.64	25.74	--
	0.9	5.58	8.43	13.44	25.40	--
	0.8	5.47	8.29	13.24	25.08	--
	0.7	5.37	8.15	13.04	24.75	--
	0.6	5.27	8.02	12.83	24.43	--
	0.5	5.16	7.86	12.63	24.11	--
30	1.0	7.45	26.74	--	--	--
	0.9	7.28	26.10	--	--	--
	0.8	7.12	25.45	--	--	--
	0.7	6.96	24.80	--	--	--
	0.6	6.79	24.16	--	--	--
	0.5	6.63	23.51	--	--	--

TABLE 5

Stability Number $N_s = \frac{\gamma z}{C_v}$ by Limit Analysis for an Anisotropic and Nonhomogeneous Soil with C_v Increasing Linearly with Depth (φ = constant)

Slope Angle (Degree) β	Anisotropy Factor K	Stability Number N_s				
		Friction Angle (Degree) ϕ=0 (m=45°)	Friction Angle (Degree) ϕ=10 (m=50°)	Friction Angle (Degree) ϕ=20 (m=55°)	Friction Angle (Degree) ϕ=30 (m=60°)	Friction Angle (Degree) ϕ=40 (m=65°)
90	1.0	2.00	2.42	2.90	3.75	4.66
	0.9	2.00	2.40	2.87	3.74	4.66
	0.8	2.00	2.38	2.85	3.73	4.65
	0.7	2.00	2.38	2.85	3.72	4.64
	0.6	2.00	2.38	2.85	3.72	4.64
	0.5	2.00	2.38	2.85	3.71	4.63
70	1.0	2.83	3.68	4.74	6.73	9.81
	0.9	2.77	3.54	4.68	6.63	9.76
	0.8	2.74	3.53	4.65	6.43	9.71
	0.7	2.73	3.51	4.63	6.40	9.66
	0.6	2.71	3.49	4.61	6.36	9.60
	0.5	2.69	3.47	4.58	6.33	9.55
50	1.0	3.94	5.44	8.62	15.50	--
	0.9	3.85	5.35	8.45	15.23	--
	0.8	3.76	5.26	8.28	14.96	--
	0.7	3.61	5.16	8.10	14.69	--
	0.6	3.52	5.06	7.93	14.42	--
	0.5	3.45	4.95	7.76	14.09	--
30	1.0	5.47	19.33	--	--	--
	0.9	5.31	18.72	--	--	--
	0.8	5.14	18.11	--	--	--
	0.7	4.98	17.50	--	--	--
	0.6	4.82	16.89	--	--	--
	0.5	4.66	16.28	--	--	--

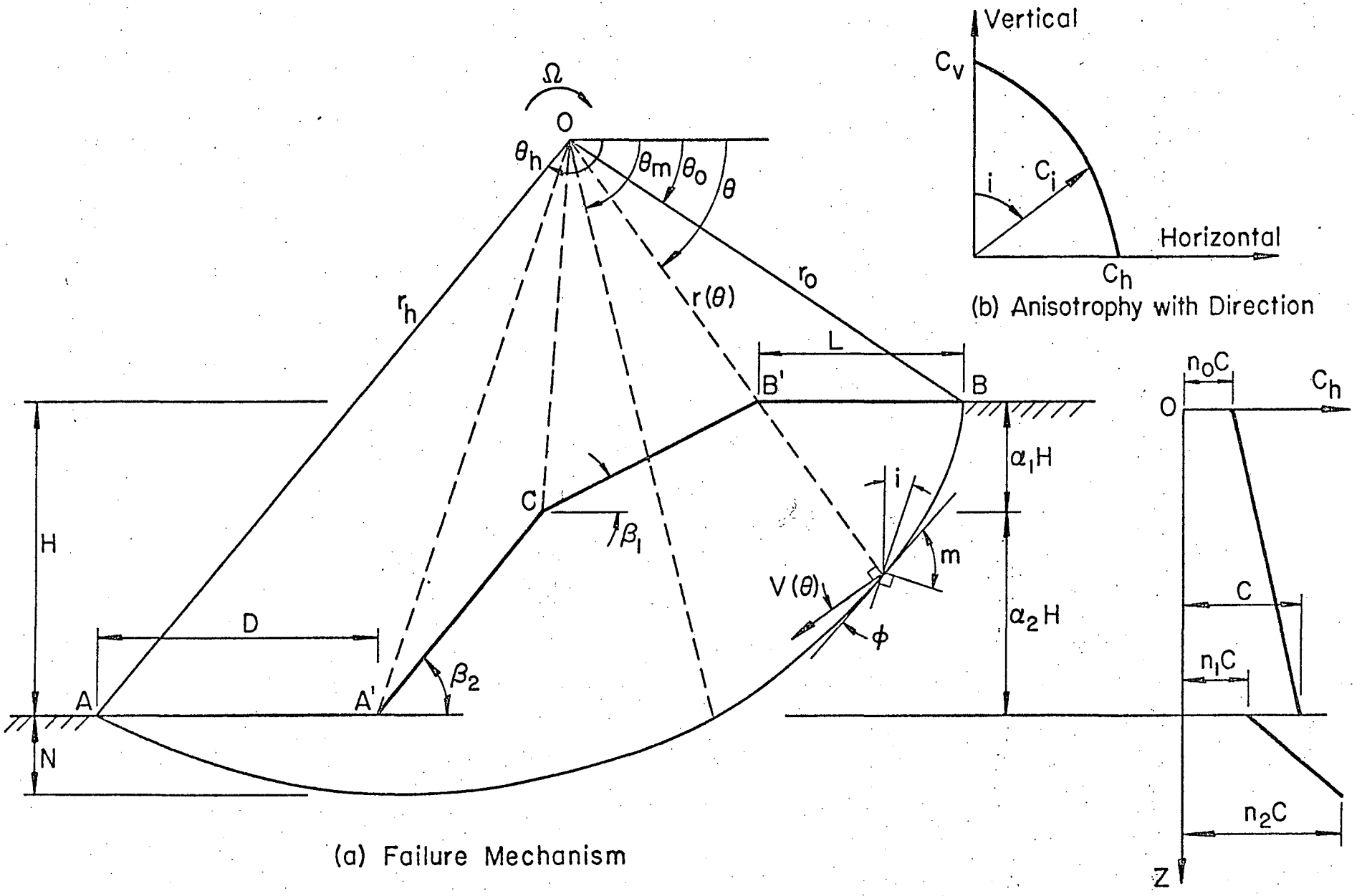

Fig. 1 A Log-Spiral Failure Mechanism

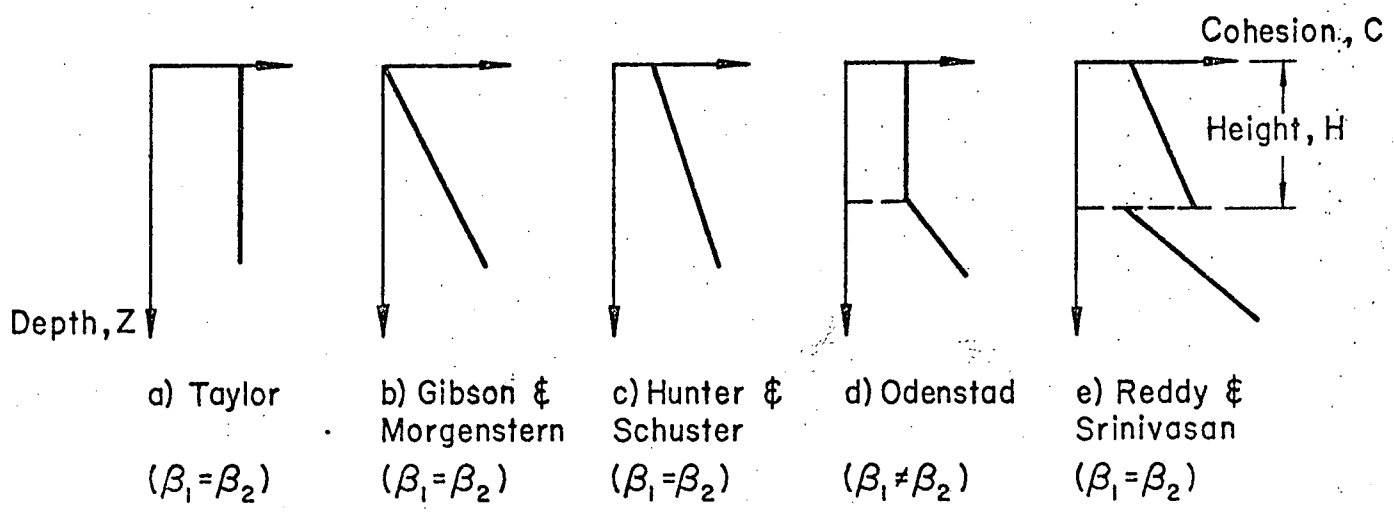

Fig. 2 Several Forms of Cohesion Stress Distributions